Global Dirac phenomenology for proton elastic scattering from ^{4}He

B. C. Clark
Department of Physics, The Ohio State University Columbus, Ohio 43210, USA

E. D. Cooper
Department of Physics, University College of the Fraser Valley, Abbotsford, British Columbia V2S 7M6, Canada

S. Hama
Hiroshima University of Economics, Hiroshima 731-0192, Japan

(Received 10 October 2005; published 27 February 2006)

In the past, Dirac phenomenology has been used to determine global proton-nucleus optical potentials for a number of targets. ^{4}He has not been previously included in these analyses. This paper addresses $p + {}^4$He using medium-energy proton elastic scattering data with proton kinetic energies in the laboratory from 156 to 1728 MeV. The characteristic features of the optical potentials for $p + {}^4$He are shown as well as the the predictive power of the global approach for this nucleus.

DOI: 10.1103/PhysRevC.73.024608 PACS number(s): 25.40.Cm, 24.10.Jv, 24.10.Ht

I. INTRODUCTION

For several years Dirac phenomenology has been used to determine global proton-nucleus optical potentials that span energies from 20 to 1040 MeV [1,2]. Previously, ^{4}He has been left out, so here we present a global optical potential for $p + {}^4$He in the energy range from 156 to 1728 MeV. The scalar-vector (SV) model of Dirac phenomenology used in Hama *et al.* [1] and Cooper *et al.* [2] is used in this paper. The Coulomb potential, V_c, is determined from the empirical charge distribution [3]. The reason why we did not produce a fit for ^{4}He in the past was because it was a surprisingly difficult task. However, we have now found a fit that we believe to be respectable enough to share, so we are presenting it here. The parametrization of the fit looks a little unusual because of the way we have had to constrain the parameters.

II. PARAMETRIZING THE POTENTIALS

We parametrize vector and scalar potentials that go into a Dirac equation, which is then solved for scattering solutions. The Dirac equation is

$$\{\alpha \cdot \mathbf{p} + \beta[m + U_s(r)] + [U_0(r) + V_c(r)]\}\Psi(\mathbf{r}) = E\Psi(\mathbf{r}). \tag{1}$$

The scalar and vector potentials are both parametrized as

$$U_j(r, E) = V_j(E) f_j(r, E) + iW_j(E) g_j(r, E), \tag{2}$$

where the subscript j can be s for scalar or 0 for vector, respectively. Because we consider only proton data we did not include a term dependent on isospin, which should be small for ^{4}He. The geometries were taken to be symmetrized Woods-Saxon (SWS) shapes with a fourth-order polynomial in the numerator:

$$f_j \text{ and } g_j = \left\{\left[1 + \exp\frac{[r - R(E)]}{a(E)}\right]^{-1} \times \left[1 + \exp\frac{-[r + R(E)]}{a(E)}\right]^{-1}\right\} \times \left[1 + \frac{w_1 r2}{R2(E)} + \frac{w_2 r4}{R4(E)}\right]. \tag{3}$$

As in the work of Hama *et al.* [1] and Cooper *et al.* [2] the Cooper-Jennings recoil factors [4] were employed for both scalar and vector potentials, including V_c. The two factors R_s and R_v multiply the Lorentz scalar and vector optical potentials, respectively, and can be thought of as a relativistic version of a reduced mass. The factor R_s is

$$R_s = (\text{target mass})/\sqrt{s}, \tag{4}$$

where $\sqrt{s}$ is the total c.m. energy of p-A system. The corresponding recoil factor for the vector potential is

$$R_v = (\text{total c.m. energy of target})/\sqrt{s}. \tag{5}$$

These factors multiply the scalar U_s and vector $U_0 + V_c$ potentials in the Dirac equation.

Recoil effects are presumably large in ^{4}He and are accounted for by these factors. However, since we search only on the strengths of the potentials in this approach, their presence here is more of a formality.

We were unable to obtain satisfactory fits to the data using a simple Woods-Saxon form, or SWS form. This was discussed in the case of a single energy fit at 500 MeV by Moss *et al.* [5] and Greben and Gourishankar [6]. The simplest way to go beyond this form is to put a polynomial in the numerator; we found that going to fourth order gave us sufficient flexibility. We did not find it necessary to introduce an energy dependence to the two coefficients w_1 and w_2.

The expression for the potential used here has several parameters that themselves are parametrized as functions of energy. Because we expect them to be changing less quickly with energy at higher energies than at lower energies, we parametrize our strength and geometry parameters in terms of the variable $x = 1000/E^p_{\text{c.m.}}$, where $E^p_{\text{c.m.}}$ is the proton's total relativistic energy (mass energy + kinetic) in the center of momentum frame. This is the same approach used in Refs. [1,2]. In practice we found that powers up to x^3 were adequate for this energy range.

III. DETAILS OF PRODUCING THE FIT

We initially hoped that a simple approach that works on heavier nuclei would swiftly deliver a good optical potential for ^{4}He. However, we found that if left unguided the fitting procedure produced potentials that had large imaginary parts (several hundred MeV). This feature was quite robust, but at the present time we can think of no physical mechanism to explain it. We suspect it to be an artifact of the data used. The small size of the nucleus means that the differential cross section data have less structure than would be so for a larger nucleus. The data set is less extensive than that of heavier nuclei, it tends to be older, and there are fewer data points with larger error bars and there is not so much spin observable data.

Perhaps as a consequence of these three points, we found that fitting the data is no guarantee of reasonable looking potentials or of reasonable looking reaction cross sections. Moreover, we found that fitting $\sigma(\theta)$ and A_y data did not give an automatic fit to the other spin observables (the R parameter at 500 MeV [6] in this case). This contrasts with our experience on heavier nuclei.

To simply take each parameter to be a cubic function of x and allow the computer to go to work was disastrous. The potentials produced seemed quite unphysical. To obtain the fit was a tedious process of trial-and-error constraining of the potentials. In the end we found it necessary to impose some constraints.

We constrained the imaginary scalar potential to be

$$W_S(r, E) = 125x^{0.25}. \tag{6}$$

We also constrained the difference between the real scalar and vector potentials to be

$$D_R = V_0 - V_S = x^{0.8}(c_1 + c_2 x), \tag{7}$$

where c_1 and c_2 are adjusted parameters, and also constrained $w_1 = 0.25$ and $w_2 = 0$ for the imaginary scalar potential. The sum of the real scalar and vector potentials, $S_R = V_0 + V_S$, is simply taken to be a cubic function of x. These constraints then gave us potentials that resembled those we would expect from the impulse approximation, or those we got while doing unconstrained fits on heavier nuclei. Specifically, it gave us imaginary potentials between 50 and 100 MeV in strength, consistent with those we had previously obtained in fits to other nuclei where we did not need to impose this constraint by hand. This constraint also allowed "reasonable" reaction cross section predictions, as opposed to reaction cross sections that sometimes even went negative at the lowest energy with the unconstrained fits.

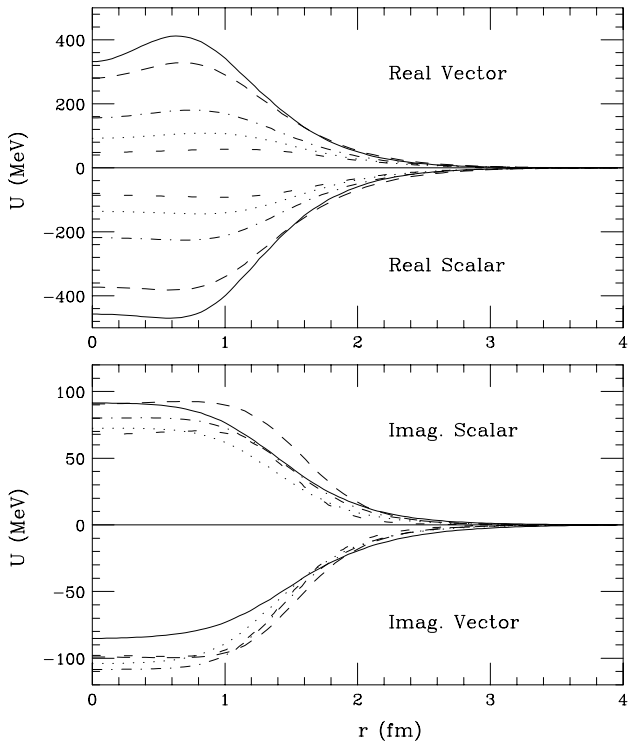

FIG. 1. The potentials as a function of energy. The solid line is at 200 MeV, the dashed line is at 350 MeV, the dash-dot line is at 800 MeV, the dotted line is at 1240 MeV, and the spaced-out dashed line is at 1728 MeV.

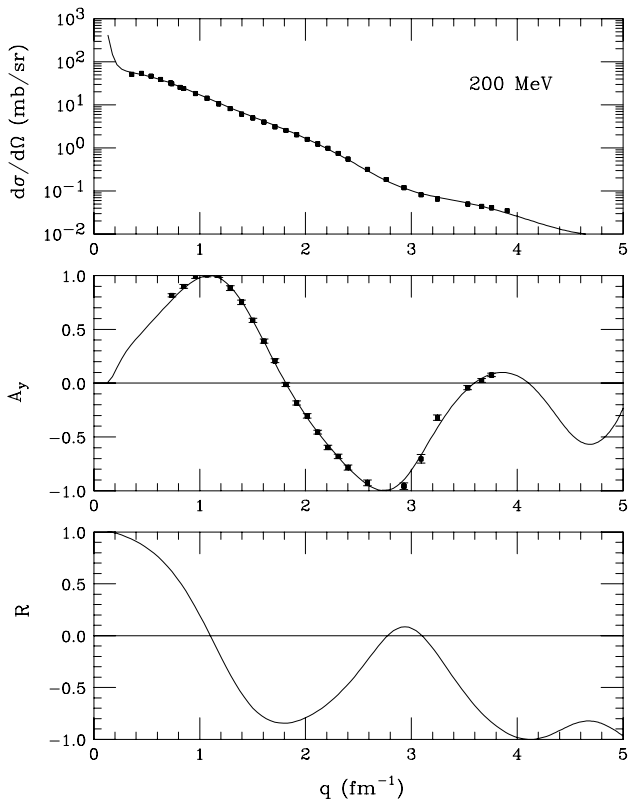

FIG. 2. The results for $p + ^4$He at 200 MeV. The data are from Ref. [5].

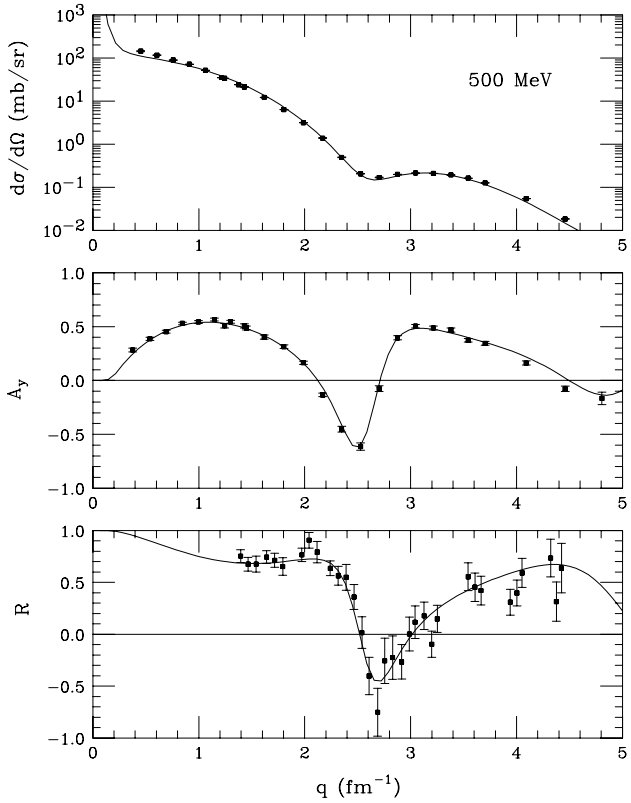

FIG. 3. The results for $p + {}^4$He at 500 MeV. The data are from Ref. [6].

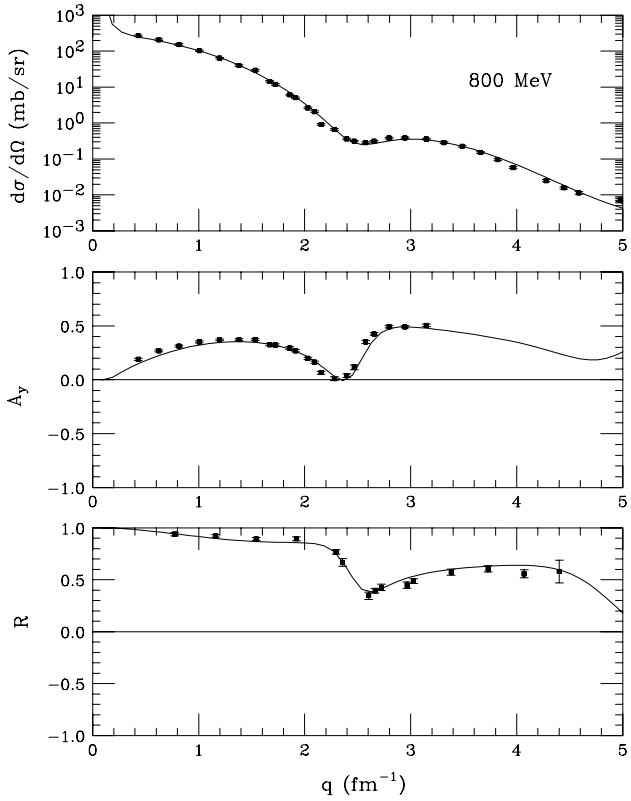

FIG. 4. The results for $p + {}^4$He at 800 MeV. The data are from Refs. [10–12].

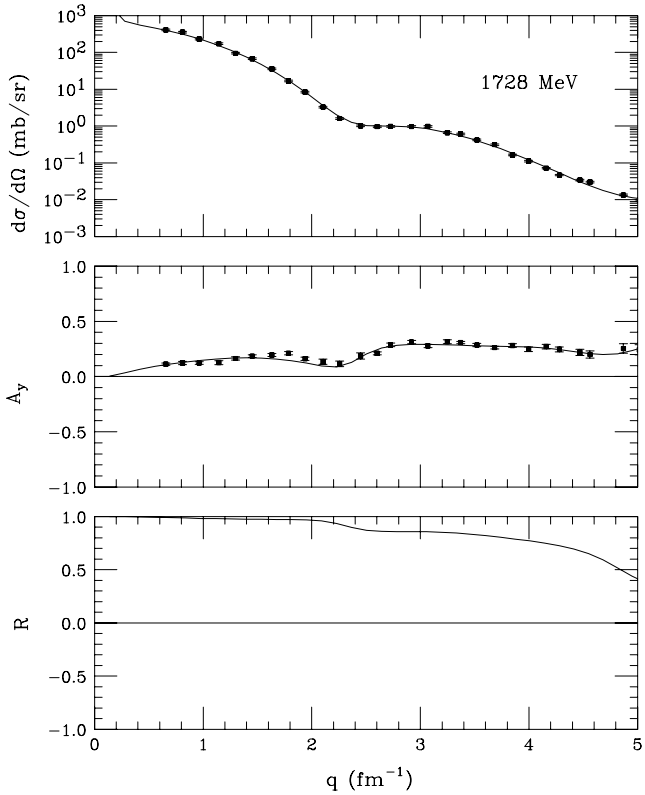

FIG. 5. The results for $p + {}^4$He at 1728 MeV. The data are from Refs. [11,12].

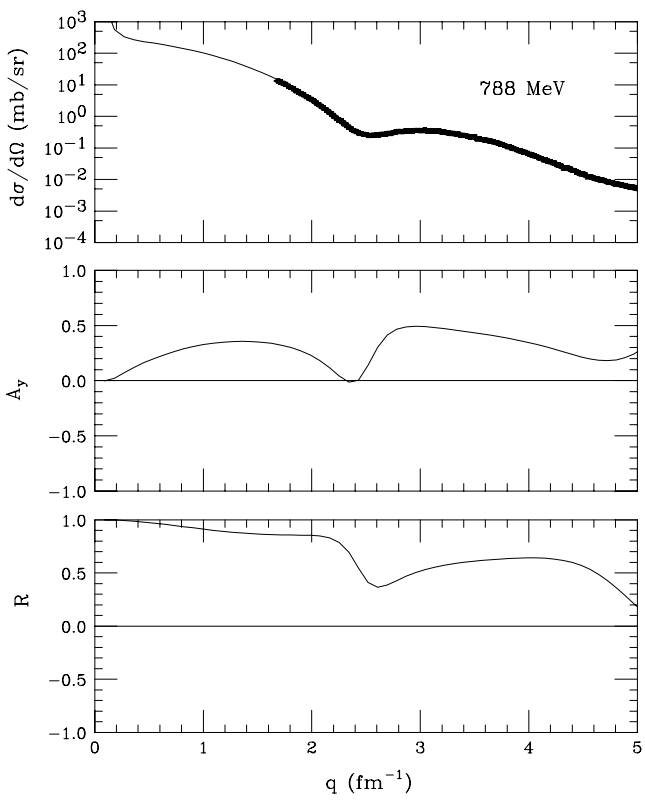

FIG. 6. The predictions for $p + {}^4$He at 788 MeV. The data are from Ref. [13].

TABLE I. Potential parameters of best fit.

x	$= 1000/E^{p}_{\text{c.m.}}$
S_R	$= -978.5503603 + 4316.904390x - 6608.849154x^2 + 3231.566144x^3$
D_R	$= -875.2315053x^{0.8} + 2232.447037x^{1.8}$
Real Vector	
V_0	$= (S_R + D_R)/2$
R	$= 8.617616893 - 29.84965759x + 37.88503845x^2 - 16.39919464x^3$
a	$= 0.786091018 - 2.076885320x + 3.035244766x^2 - 1.435519343x^3$
w_1	$= 0.9967839657$
w_2	$= -0.03090937349$
Imag. Vector	
W_0	$= 50.79424956 - 579.6270433x + 380.1128566x^2 + 54.69695846x^3$
R	$= 11.70038533 - 46.18432913x + 63.90965243x^2 - 28.86857144x^3$
a	$= -3.646922078 + 16.51799610x - 23.01720173x^2 + 10.53173074x^3$
w_1	$= 0.1331521091$
w_2	$= 0.2842912264$
Real Scalar	
V_s	$= (S_R - D_R)/2$
R	$= 2.927371087 - 6.267362964x + 5.421153798x^2 - 1.538166556x^3$
a	$= 1.203172799 - 3.820557035x + 5.233705616x^2 - 2.406689149x^3$
w_1	$= 0.4205562336$
w_2	$= 0.4074032181$
Imag. Scalar	
W_s	$= 125x^{0.25}$
R	$= 14.99124087 - 60.15737738x + 83.72437219x^2 - 38.06370158x^3$
a	$= -7.959644910 + 34.05359443x - 46.26205326x^2 + 20.64969278x^3$
w_1	$= 0.25$
w_2	$= 0.0$

The rest of the parameters were then expressed as simple polynomials in x. Note that in this paper we are fitting a total number of 584 data points with 48 parameters. With fewer parameters we could not get a good description of the data; with additional parameters there were too many local chi-squared minima and the fit tended to produce unphysical potentials. Even with the constraints described here, the chi-squared space still has many minima. The technique that seemed the most effective in finding a good minimum was to start with reasonable looking parameters and obtain a fit using the Marquadt algorithm [7]. Then take the starting values and randomly multiply them with random numbers near 1 and re fit the data. Often the best fit would emerge after 50 or 100 trials, which is a testament to the nonlinear nature of this fitting procedure.

The elastic data itself were edited for the purpose of this fit. At larger angles nonlocalities in the potential, including those from triton exchange, become important. Trying to fit these with a local potential is possible but would be a mistake. Thus we have cut off the data we use in this fit at 110 degrees. Also, since there is much more cross section data than spin observable data we weighted more heavily the analyzing power and spin rotation parameter data at 200, 350, 500, 800, 1240, and 1720 MeV.

IV. RESULTS

We have used 14 data sets. Ten were used in the fit, and four were used to check the interpolation properties of the fit. The 10 used were 156 MeV from Comparat *et al*. [8]; 200, 350, and 500 MeV from Moss *et al*. [5]; 500 MeV [6]; 650 MeV [9]; and 561, 800, 1029, 1240, and 1728 MeV [10–12]. The four used to check the interpolation were 544 MeV [9], 587 MeV [9], 788 MeV [13], and 1050 MeV [14].

Table I shows the parameters we found that gave our best fit.

Figure 1 shows the scalar and vector global optical potentials we have obtained for $p + {}^4$He for five different incident proton energies: 200, 350, 800, 1240, and 1728 MeV. Figures 2–4 show the fits to the $p + {}^4$He elastic cross section (σ), analyzing power (A_y), and Wolfenstein (R) parameter. At 800 MeV the cross section and analyzing power data were used in the fit, but the R-parameter data were found only afterward so this is actually a prediction for the R-parameter data. The prediction is excellent.

Figure 6 shows the prediction for the cross section at 788 MeV, where data exist but were left out of the fitting process. The fit is good out to the same momentum transfer as was fit at 800 MeV, then it drifts away from the data. We have also checked that the reproduction of the analyzing power data at 544 MeV and the cross section data at 587 MeV is satisfactory despite those data sets also not being included in the search. There is a picture of analyzing power data taken at 560 MeV in Ref. [11] that differs from that at 544 MeV by having sharper maxima and minima; our prediction for these data appears to agree even better than for the 544-MeV data,

TABLE II. Reaction cross sections.

E_{Lab} (MeV)	σ_R (fm^2)
156.0	15.058
200.0	10.230
350.0	7.311
500.0	7.759
544.0	7.746
587.0	7.903
561.0	7.807
650.0	8.143
788.0	8.688
800.0	8.735
1029.0	9.449
1050.0	9.488
1240.0	9.584
1728.0	8.736

which is reassuring since the newer data from Ref. [11] were taken with detectors that had a smaller angular resolution. The shape of the cross section data at 1050 MeV is well reproduced; however, the normalization of the data appears inconsistent with that of the other data sets used.

Table II shows the reaction cross sections obtained from fitting the elastic data. We note that the reaction cross section at 156 MeV seems unrealistically high. However, at all the other energies we have used, all our somewhat-decent fits tend to produce the same reaction cross section prediction. Presumably the problem at 156 MeV comes about because not only is it at the end of the energy range, but also the cross section data used at 156 MeV has very little structure up to 110 degrees, and there are no spin observables. We, therefore, caution the user about using this global fit for reaction calculations below 200 MeV.

V. CONCLUSION

In this paper we have presented a global Dirac $p + {}^4$He optical potential in the range from 156 to 1728 MeV. The quality of the fits is good, and the interpolation (prediction) properties are good. However, we had to constrain the potentials to resemble those we would expect from fits to heavier nuclei. The fit presented here is available from bcc@mps.ohio-state.edu, coopert@ucfv.ca, and sn-hama@hue.ac.jp.

ACKNOWLEDGMENT

This work was supported in part by the National Science Foundation under Grant Nos. PHY-0098645 and PHY-0354916.

[1] S. Hama, B. C. Clark, E. D. Cooper, H. S. Sherif, and R. L. Mercer, Phys. Rev. C **41**, 2737 (1990).
[2] E. D. Cooper, S. Hama, B. C. Clark, and R. L. Mercer, Phys. Rev. C **47**, 297 (1993).
[3] H. D. Vries, C. W. De Jager, and C. De Vries, At. Data Nucl. Data Tables **36**, 495 (1987).
[4] E. D. Cooper and B. K. Jennings, Nucl. Phys. **A483**, 601 (1988).
[5] G. A. Moss, L. G. Greeniaus, J. M. Cameron, D. A. Hutcheon, R. L. Liljestrand, C. A. Miller, G. Roy, B. K. S. Koene, W. T. H. van Oers, A. W. Stetz, A. Willis, and N. Willis, Phys. Rev. C **21**, 1932 (1980).
[6] J. M. Greben and R. Gourishanker, Nucl. Phys. **A445**, 445 (1983).
[7] D. W. Marquadt, J. Soc. Ind. Appl. Math. **2**, 431 (1963).
[8] V. Comparat, R. Frascaria, N. Fujiwarar, N. Marty, M. Morlet, P. G. Roos, and A. Willis, Phys. Rev. C **12**, 251 (1975).
[9] E. T. Boschitz, W. K. Roberts, J. S. Vincent, M. Belcher, K. Gotow, P. C. Perdrisat, L. W. Sewnson, and J. R. Priest, Phys. Rev. C **6**, 457 (1972).
[10] M. Geso, D. Adams, J. Bysterisky, G. Igo, A. Ling, C. Whitten, M. Nasser, L. C. Smith, and R. W. Whitney, Phys. Rev. C **58**, 3742 (1998).
[11] R. Klem, G. Igo, R. Talaga, A. Wriekat, H. Courant, K. Einsweiler, T. Joyce, H. Kagan, Y. Makdisi, M. Marshak, B. Mossberg, E. Peterson, K. Ruddick, and T. Walsh, Phys. Rev. Lett. **38**, 1272 (1977).
[12] R. Klem, G. Igo, R. Talaga, A. Wriekat, H. Courant, K. Elinsweiler, J. Joyce, H. Kagan, Y. Makdisi, M. Marshak, B. Mossberg, E. Peterson, K. Ruddick, and T. Walsh, Phys. Lett. **B70**, 155 (1977).
[13] H. Courant, K. Einsweiler, T. Joyce, H. Kagan, Y. I. Makdisi, M. L. Marshak, B. Mossberg, E. A. Peterson, K. Ruddick, T. Walsh, G. J. Igo, R. Talaga, A. Wriekat, and R. Klem, Phys. Rev. C **19**, 104 (1979).
[14] D. Baker, R. Beurtey, G. Burge, A. Chaumeaux, J. M. Durand, J. C. Faiver, J. M. Fontaine, G. Garreta, D. Lergrand, J. Saudinos, J. Thirion, R. Bertini, F. Brochard, and F. Hibou, Phys. Rev. Lett. **32**, 836 (1974).